Genomic surveillance of Nevada patients revealed prevalence of unique SARS-CoV-2 variants bearing mutations in the RdRp gene

Paul D. Hartley[1,4*], Richard L. Tillett[7*], David P. AuCoin[3,4], Joel R. Sevinsky[6], Yanji Xu[4,5], Andrew Gorzalski[2,4], Mark Pandori[2,4], Erin Buttery[8], Holly Hansen[8], Michael A. Picker[8], Cyprian C. Rossetto[3,4*#], Subhash C. Verma[3,4*#]

Affiliations:

[1] Nevada Genomics Center

[2] Nevada State Public Health Laboratory

[3] Department of Microbiology & Immunology, University of Nevada, Reno School of Medicine

[4] University of Nevada, Reno

[5] Nevada Center for Bioinformatics

[6] Theiagen Consulting, LLC

[7] Nevada Institute of Personalized Medicine, University of Nevada, Las Vegas,

[8] Southern Nevada Public Health Laboratory of the Southern Nevada Health District, Las Vegas

* These authors contributed equally to this work and are listed in alphabetical order

[#] To whom correspondence should be addressed:

Cyprian C. Rossetto crossetto@med.unr.edu, Subhash C. Verma scverma@med.unr.edu

Running title: Unique RdRp variant of SARS-CoV-2 in Nevada patients

Keywords: SARS-CoV-2, COVID-19, genome enrichment, nsp12, RdRp, orf1b 314

ABSTRACT:

Patients with signs of COVID-19 were tested with CDC approved diagnostic RT-PCR for SARS-CoV-2 using RNA extracted from nasopharyngeal/nasal swabs. In order to determine the variants of SARS-CoV-2 circulating in the state of Nevada, 200 patient specimens from COVID-19 patients were sequenced through our robust protocol for sequencing SARS-CoV-2 genomes. Our protocol enabled sequencing of SARS-CoV-2 genome directly from the specimens, with even very low viral loads, without the need of culture-based amplification. This allowed the identification of specific nucleotide variants including those coding for D614G and clades defining mutations. These sequences were further analyzed for determining SARS-CoV-2 variants circulating in the state of Nevada and their phylogenetic relationships with other variants present in the united states and the world during the same period of the outbreak. Our study reports the occurrence of a novel variant in the nsp12 (RNA dependent RNA Polymerase) protein at residue 323 (314aa of orf1b) to Phenylalanine (F) from Proline (P), present in the original isolate of SARS-CoV-2 (Wuhan-Hu-1). This 323F variant is found at a very high frequency (46% of the tested specimen) in Northern Nevada. Functional significance of this unique and highly prevalent variant of SARS-CoV-2 with RdRp mutation is currently under investigation but structural modeling showed this 323aa residue in the interface domain of RdRp, which is required for association with accessory proteins. In conclusion, we report the introduction of specific SARS-CoV-2 variants at a very high frequency within a distinct geographic location, which is important for clinical and public health perspectives in understanding the evolution of SARS-CoV-2 while in circulation.

50 **INTRODUCTION:**

51 Severe Acute Respiratory Syndrome coronavirus 2 (SARS-CoV-2), the cause of
52 coronavirus disease 2019 (COVID-19), was first identified and reported in December
53 2019 in Wuhan, Hubei province, China [1-3]. RNA sequencing and phylogenetic analysis
54 of specimens taken during the initial outbreak in Wuhan determined that the virus is most
55 closely related (89.1% nucleotide similarity) to a group of SARS-like coronaviruses (genus
56 Betacoribavirus, subgenus Sarbecovirus) which had previously been identify in bats in
57 China [4,2]. Coronaviruses have a recent history as emerging infections, first SARS-CoV
58 in 2002-2003, and Middle East respiratory syndrome coronavirus (MERS-CoV) in 2012,
59 both zoonotic infections that cause severe respiratory illness in humans [5,6,2,7,8] [2,5-
60 8]. Unlike SARS-CoV and MERS-CoV which displayed limited global spread, SARS-CoV-
61 2 has spread around the world within a few months. There are specific characteristics of
62 SARS-CoV-2 which have facilitated the transmission, including infections that result in
63 asymptomatic or mild disease, allowing for under-characterized transmission.

64 SARS-CoV-2 is an enveloped, positive single-stranded RNA virus. Detection of
65 SARS-CoV-2 in patients has primarily occurred using RT-qPCR to detect viral RNA from
66 respiratory specimens (primarily nasal and nasopharyngeal swabs). While RT-PCR
67 results can be quantified through determination of a cycle threshold (Ct) value for each
68 sample, it does not yield sequence data leading to the description of genomic variants.
69 To further study of such variants, and to better understand the epidemiology of the virus
70 in the state of Nevada, we developed a workflow that allowed us to sequence SARS-CoV-
71 2 genomic RNA from patient swabs containing a broad range of viral loads. Of the
72 sequences of SARS-CoV-2 currently submitted to common database (GenBank and

73 GISAID), several were obtained after the virus had been passed in Vero cells [9,10] and
74 others came directly from patient specimens [11,12]. Certain data have suggested a
75 potential for lab acquired mutations following passage in cell culture [13,9]. Specifically,
76 a report of SARS-CoV-2 passage in Vero cells which resulted in a spontaneous 9 amino
77 acid deletion within the spike (S) protein that overlaps with the furin cleavage site [13].
78 The loss of this site is suggested to increase the viral entry into Vero cells [14]. For both
79 research and epidemiological purposes, sequencing of SARS-CoV-2 directly from patient
80 specimens not only reduces the possibility of laboratory acquired mutations following
81 passage in cell culture but also reduces the time that would be spent growing the virus
82 from the patient specimens and subsequently also reduces handling larger amounts of
83 infectious virus. Additionally, one of the goals in developing an optimized SARS-CoV-2
84 NGS protocol was to be able to generate adequate depth of coverage of the viral genome
85 while minimizing the sequencing of non-viral RNA which would allow for more specimens
86 to be multiplexed together during sequencing.

87 Our workflow employs a combination of RNA amplification, conversion into
88 Illumina-compatible sequencing libraries and enrichment of SARS-CoV-2 library
89 molecules prior to sequencing. Using this novel methodology, we sequenced SARS-
90 CoV-2 from a total of 200 patient specimens collected over a three-month period
91 originating from Nevada. Of the 200 selected, 173 were sequenced with enough quality
92 to be used for determining SARS-CoV-2 nucleotide variants to perform further
93 phylogenetic analysis and study the viral epidemiology within the state of Nevada.
94 Analysis of the data suggests a specific epidemiological course for the local epidemic
95 within Northern Nevada. This was characterized by an initial observation of variants

96 closely resembling isolates originating directly from China or Europe. Subsequent to
97 government-mandated period of restrictions on business and social activity, we observed
98 that a viral isolate not seen elsewhere in the world emerged within Northern Nevada cases
99 (nucleotide 14,407 and 14,408). This isolate contains an amino acid change in residue
100 P323L/F of RdRp (nsp12). Furthermore, we found that sampled viral isolates in Southern
101 Nevada, unlike those in Northern Nevada, closely resembled the makeup of the United
102 States in general.
103
104 **MATERIALS AND METHODS:**
105 **SARS-CoV-2 specimen and library preparation.**
106 Nasal and Nasopharyngeal swab specimens were received at the Nevada State
107 Public Health Lab (NSPHL) or Southern Nevada Public Health Lab (SNPHL) and RNA
108 extraction was completed using either a QIAamp Viral RNA Mini Kit (QIAGEN) or Mag-
109 Bind Viral DNA/RNA kit (Omega Biotek). Specimens were tested for the presence of
110 coronaviral RNA using FDA-approved kits that employed RT-PCR to detect SARS-COV-
111 2 RNA.
112 A set of 200 coronavirus positive specimens were selected for genome
113 sequencing. Specimens were treated with DNase I (QIAGEN) for 30 minutes at room
114 temperature and concentrated using RNeasy Minelute spin columns (QIAGEN) based on
115 the manufacturer supplied protocol. These concentrated samples were converted into
116 Illumina-compatible sequencing libraries with a QIAseq FX Single Cell RNA Library kit
117 (QIAGEN). RNA samples were annealed to a 1:12.5 dilution of QIAseq FastSelect -HMR
118 probes (QIAGEN) to reduce subsequent amplification of human ribosomal RNA. After

119 treatment to remove trace DNA from the samples, a reverse transcription reaction was
120 carried out using random hexamers. The synthesized DNA was ligated to one another,
121 followed by isothermal linear amplification. Amplified DNA (1 μg) was enzymatically
122 sheared to an average insert size of 300 bp, and Illumina-compatible dual-indexed
123 sequencing adapters were ligated to the ends. Next, about 300 ng of adapter-ligated
124 sample was amplified with 6 cycles of PCR with KAPA HiFi HotStart polymerase (Roche
125 Sequencing Solutions). Enrichment of library molecules containing SARS-CoV-2
126 sequence was conducted with a myBaits kit and coronavirus-specific biotinylated probes
127 (Arbor Biosciences). Each enrichment used 500 ng of PCR-amplified DNA, was carried
128 out based on manufacturer instructions at a hybridization temperature of 65° for 16 hours,
129 and was completed with 8-16 cycles of PCR using KAPA HiFi HotStart polymerase.
130 Samples were sequenced using an Illumina Next-seq mid-output (2 x 75). The generated
131 FASTQ files from the sequencing reaction were analyzed as described below. The data
132 files are available at GISAID, NCBI under the
133 https://www.ncbi.nlm.nih.gov/bioproject/657893

134 **Computational analysis.**

135 Sequence pair libraries were trimmed using Trimmomatic, version 0.39 and
136 adapter-clipping setting "2:30:10:2:keepBothReads" [15]. Read pairs were aligned
137 against the Wuhan reference genome (NC_045512.2) by Bowtie 2, version 2.3.5, local
138 alignment [16]. PCR optical duplicates were removed via Picard MarkDuplicates [17].

139 Variants were called using Freebayes, version 1.0.2, with ploidy set to 1, minimum
140 allele frequency 0.75, and minimum depth of 4 [18]. No variants were called in the first
141 200 bp and final 63 bp of the COVID-19 genome. High-quality variant sites were selected

142 where site “QUAL > 20” using *vcffilter*, VCFlib version 1.0.0_rc2 [19]. Individual genomes
143 were reconstructed by their filter-passing variants using *bcftools consensus* and only
144 where aligned coverage depth ≥ 4; bases with coverage below four are reported as
145 unknown (Ns) [20].

146 A set of 3,644 complete, high-coverage SARS-CoV-2 genomes reported in the
147 July 15, 2020 Nextstrain.org global subsample and metadata were obtained from GISAID
148 and combined with our own samples to determine their phylogenetic placement [21,22].
149 Four of the global samples were set aside after screening for unexpected FASTA
150 characters. The combined sets of global and Nevadan samples were aligned together,
151 with metadata, by the *augur* phylodynamic pipelines of the *ncov* build of the *nextstrain*
152 command-line tool, version 2.0.0.post1 [23].

153 Cumulative frequency of D614G, clades (19A, 19B, 20A, 20B, 20C), and P323L/F
154 were calculated at each time point based on the total number of specimens up to the
155 indicated date. Plots and pie charts were generated using GraphPad Prism (version 8).

156 **nsp12 protein modeling.**

157 Sequence of nsp12 (RdRp) protein for SARS-CoV-2 (YP_009725307.0) was
158 retrieved from NCBI protein database and 3D model was structured based on a previously
159 published report (PDB ID: 6XEZ [24]. In addition to nsp12 (chain A), the model also
160 contains nsp7 (chain C), nsp8 (chain B and D), nsp13 (chain E and F), ligands (Zn^{2+},
161 Mg^{2+}) and RNA template and product strands. Mutational changes to residue 323 within
162 nsp12 were performed using PyMol Molecular Graphics System (version 2.0, Schrödinger
163 LLC). The original proline (P) was mutated to either leucine (L) or phenylalanine (F) as
164 indicated, these residues along with residues containing side chains within 5 Å of P323L/F

165 are shown as sticks. The rotamers for each P323L/F were assessed and those with the
166 least rotational strain and steric hindrance were used to generate the final image. To
167 determine any NCBI deposited sequences which contain the P323F variant, standard
168 protein BLAST from the BLASTp suite was used to find nsp12 protein sequences which
169 contained FSTVFP**F**TSFGP (P323F is bold and underlined) from full length SARS-CoV-
170 2 genomes. The P323F amino acid changes were confirmed with the NCBI deposited
171 nucleotide sequences.
172
173 **RESULTS:**
174 **RNA-seq workflow and assembly of SARS-CoV-2 genomes.**
175 A total of 200 SARS-CoV-2 positive specimens collected in Nevada from March 6
176 to June 5 were randomly selected to have their viral genomes sequenced for variant
177 analysis and subsequent epidemiological studies (Fig 1A and Materials & Methods). Of
178 the sequenced specimens, 173 had >90% coverage and sufficient depth to accurately
179 call those genomic positions with variants (Fig. 1B). An alignment of SARS-CoV-2
180 genomes from these specimens is presented as supplemental data (Supplemental Fig.
181 S1) showing 173 specimens with over 90% coverage. These 173 specimens represented
182 133 patient specimens from Northern Nevada (including Washoe County of which Reno
183 is the major city, the Carson-Tahoe area, and other northern, rural counties), 40 patient
184 specimens from Southern Nevada (Clark County, which encompasses Las Vegas and
185 surrounding cities). Nucleotide similarity and variants were determined and used to
186 measure the phylogenetic relationships (Supplemental Fig. S2). The combined nucleotide
187 diversity across the entire SARS-CoV-2 genome for the Nevada specimens is shown in

188 figure 1D, along with the genomic areas that were assessed for change in frequency
189 corresponding to amino acids D614G, P323L/F and nucleotide 379.

190 During the sequencing analysis we also examined the correlation between Ct
191 values from the diagnostic RT-PCR and percentage coverage of the viral genome to
192 determine the performance and robustness of our sequencing method in relation to
193 available viral RNA in a specimen of a given Ct (Fig. 1C). On average, a Ct value less
194 than 37 resulted in at least 90% coverage to the SARS-CoV-2 genome. Importantly, our
195 in-house developed method for viral genome enrichment and sequencing directly from
196 the patient's specimens (nasal and nasopharyngeal swabs) was robust and yielded
197 sequences covering over 90% of the genome even in samples having very high Ct (~40)
198 of viral genome detection. This is highly significant and shows the power of our workflow
199 in sequencing of SARS-CoV-2 genome from a spectrum of samples including the ones
200 having inadequate amounts of specimen (due to the variability in collection) or lower viral
201 loads in nasal secretions. Consequently, our sequencing protocol avoids any molecular
202 epidemiological bias, which may get acquired through cell culture-based amplification
203 especially in those specimens with high Ct (low viral load) as our method eliminates the
204 need of virus culture.

205 **Prevalence of amino acid variant D614G of SARS-CoV-2 spike protein in specimens**
206 **collected in Nevada.**

207 Earlier studies have revealed the emergence, spread and potential importance of
208 an alteration, D614G (genomic change at 23403A>G), of the spike protein [25]. This
209 missense mutation has become a clade-distinguishing locus that differentiates viral
210 isolates originating in Asia from those that have emerged from Europe. A total of 173

211 cases were analyzed to determine the number and relative proportion of the specimens
212 which carried the D614G spike protein variant in Nevada. The cumulative frequency for
213 D614 and G614 were plotted from March 6 to June 5 (Fig. 2A). Specimens from the
214 beginning of March represent the earliest known cases in Nevada, and of the 14
215 specimens sequenced during this time period (March 6-March 15) D614 was the
216 predominant variant. This shifted from March to June with an increasing frequency of the
217 G614 allele. The trend for specimens originating from either Northern Nevada (N-NV) and
218 Southern Nevada (S-NV) both show a higher frequency of G614 (Fig. 2B). We used a
219 subsampling of sequence data from Nextstrain.org to assess the frequency of D614G in
220 the United States and globally during the same time period (March 6 to June 5) (Fig. 2B
221 and 2C). The global trend by continent of D614G is also similar, with G614 at a higher
222 frequency, the one noted exception is in Asia, where D614 and G614 continue to exist in
223 equal proportions (Fig. 2C).

224 **Frequency of SARS-CoV-2 clades in Nevada.**

225 Worldwide, there are currently 5 main clades (19A, 19B, 20A, 20B, 20C) of SARS-
226 CoV-2 differentiated based on specific nucleotide profiles in the Year-letter scheme of
227 https://clades.nextstrain.org. Clade 19A and 19B are defined by C8782T and T28144C,
228 respectively. 20A is a derivative of 19A and contains mutations C3037T, C14408T and
229 A23403G (resulting in D614G). 20B is defined by mutations G28881A, G28882A and
230 G28883C, and 20C contains C1059T and G25563T [26].

231 To assess the introduction and spread of the clades in Nevada the cumulative
232 frequency for the clades were plotted from March 6 to June 5 (Fig. 3A). The earliest
233 sequenced specimens from Nevada were collected in the beginning of March (March 6-

234 March 15) and are predominantly from clades 19A and 19B. Additional sequenced
235 specimens collected from March to June revealed a shift to a higher frequency of 20C
236 (Fig. 3A). We performed phylogenetic reconstruction of the Nevada specimens and
237 differentiated the clades on the circular dendrogram by color (Fig. 3B). There were
238 discordant trends in the dominant clade for specimens originating from either Northern
239 Nevada (N-NV) and Southern Nevada (S-NV) (Fig. 3C and 3D). Specimens from Northern
240 Nevada (Washoe County, Carson-Tahoe, and other counties) showed a prevalence of
241 20C, while the Southern Nevada specimens from Clark County had a larger proportion of
242 20A (Fig. 3C and Supplemental Fig. S3a). We used a subsampling of Nextstrain.org data
243 to assess the frequency of clades in the United States and globally by continent during
244 the same time period (March 6 to June 5). The dominant clade in the United States was
245 20C, similar to the frequency seen in the total Nevada samples (N-NV and S-NV) (Fig.
246 3A and 3C). The global clade distributions were variable in areas outside of Asia while
247 clades 19A and 19B are noted to be more prevalent in Asia. (Fig. 3D).

248 **Prevalence of amino acid variant P323L/F of SARS-CoV-2 nsp12 (RdRp) in Nevada.**

249 Analysis of sequencing data revealed a novel observation for our specimens at
250 bases 14,407 and 14,408 which results in a change at residue 323 in nsp12 (RdRp). For
251 the Wuhan isolate at 14,407 and 14,408 there is CC for proline (P), the variants have CT
252 for leucine (P323L) and TT for phenylalanine (P323F). To assess the introduction and
253 spread of P323L/F in Nevada, the cumulative frequency of P323, L323 and F323 were
254 plotted from March 6 to June 5 (Fig. 3A). Nevada specimens from the beginning of March
255 (March 6-March 15) showed P323 to be the predominant variant. As additional specimens
256 were collected and sequenced from March to June there was a shift to a higher frequency

257 of L323 and F323 (Fig. 4A). We performed phylogenetic reconstruction of the Nevada
258 specimens and noted the P323L/F variants on the circular dendrogram with the indicated
259 colors (Fig. 4B). Interestingly, analysis of the Northern Nevada and Southern Nevada
260 specimen showed very different dominant variants (Fig. 4B). In Northern Nevada the
261 F323 was more prevalent, while in Southern Nevada L323 was more prevalent. We used
262 a subsampling of Nextstrain.org data to assess the frequency of P323L/F in the United
263 States and globally during the same time period (March 6 to June 5). P323 was the
264 predominant variant in Asia, while L323 was more prevalent in other areas of the world
265 and F323 was only appreciably noted in North America (Fig. 4D and 4E).

266 While we are investigating the phenotypic significance of this predominant variant
267 of RdRp, we performed in-silico structural modeling of RdRp to determine the spatio-
268 temporal location of this 323aa on RdRp in complex with its accessory proteins, nsp7,
269 nsp8 and nsp3. Our data showed the location of 323aa in the interface domain of RdRp
270 and variation of P323 to L or F did not significantly change the conformation of the protein
271 (Fig. 5). Since the interface domain (aa 251-398) acts as a protein-interaction junction
272 for the finger domain of the polymerase and the second subunit of nsp8 (accessory
273 protein), required for the polymerase activity, we anticipate this mutation to have
274 phenotypic effect on the RdRp activity. This suggested that P323 variants of RdRp may
275 have altered phenotype with fitness advantage/disadvantage in transmission or
276 pathogenicity and pending investigation will provide confirmatory results on this highly
277 prevalent mutation.

278

279

280 **DISCUSSION:**

281 We have developed a novel method, which combines specific depletion and
282 enrichment strategies that results in efficient SARS-CoV-2 RNA-seq with high genome
283 coverage and depth. An advantage of this protocol is that it generates sequence data
284 directly from swab specimens without the need to passage the virus in cell culture thereby
285 reducing the handling of infectious material and induction of culture-acquired mutations.
286 Another obstacle in sequencing directly from swab specimens is that most FDA-approved
287 commercially available RNA extraction kits are specifically optimized to recover low
288 amounts of total nucleic acids, include carrier polyA RNA that could be convertible into
289 sequence able molecules, as has been observed previously with RNA-seq of Lassa- or
290 Ebola-positive clinical specimens [27].

291 The workflow incorporates amplification of low-abundance RNA into micrograms
292 of DNA, followed by conversion from a fraction of the DNA into Illumina-compatible
293 sequencing libraries and enrichment of these libraries for SARS-CoV-2 sequences. In
294 addition, during the reverse transcription step a reagent was incorporated to reduce the
295 subsequent amplification of host ribosomal RNA. This approach is robust in that it
296 converts low amounts of RNA into microgram quantities of DNA representative of all the
297 RNA species (aside of rRNA) present in the specimen. This DNA can be stored
298 indefinitely to be interrogated by multiple techniques at a later date. Additionally, RNA
299 amplification is likely less sensitive to low viral abundance compared to RT-PCR. Finally,
300 the use of probes to enrich for coronavirus-specific sequencing library molecules is less
301 sensitive to variants compared to tiling PCR amplicon approaches [28-32].

302 The data herein implicate that early in the pandemic, before the “stay-at-home”
303 order on April 1st, there were multiple introductions of SARS-CoV-2 into the state of
304 Nevada. From April 1st to the beginning of June, Nevada experienced a period of semi-
305 isolation, as the casinos and most hotels shut down, tourism and travel to the state
306 essentially stopped. Because of the stay-at-home order and social distancing measures
307 put in place, there was less mobility of people within and between states. It is possible
308 that these measures, compounded by potential inherent transmission variability of some
309 viral isolates, influenced the change in the frequency of D614G, clades and P323L/F that
310 we noted during this time period within Nevada. In addition, we also found 379C>A with
311 a high prevalence in our study specimens compared to the subsampling of sequences
312 from the United States and globally (Figure 6). This is a synonymous mutation in nsp1,
313 hence the biological relevance of this nucleotide variant remains to be elucidated.
314 We found the overall trend of D614G in Nevada during this time period to be similar
315 with what was observed in other states and internationally, with the exception of within
316 Asia where the D614 allele had originated. We noted that there were differences between
317 Northern Nevada and Southern Nevada. In Northern Nevada clade 20C and F323 were
318 more frequent, while during this same time period in Southern Nevada clade 20A and
319 L323 were more prevalent. These data indicate that there were distinct genomic profiles
320 of the SARS-CoV-2 viruses that were circulating in these populations during the initial
321 months of the pandemic while stay-at-home order were in place to help prevent
322 transmission of the virus.
323

324 Of the 14,885 complete SARS-CoV-2 genomes available (as of August 14, 2020)
325 in NCBI there are only 6 genomes that have the P323F variant (accession number:
326 MT706208, LR860619, MT345877, MT627429, MT810889, MT811171). In this study 62
327 of the 133 specimens from Northern Nevada contain P323F. That is 46% of specimens
328 from Northern Nevada contained P323F compared to 0.04% of NCBI deposited SARS-
329 CoV-2 isolates. This was a significant accumulation of one specific SARS-CoV-2 variant
330 in Northern Nevada, which could have been because of the circulation of this unique
331 variant in the community without the introduction of new variants restricted by the shelter
332 in place orders. However, regardless of the confined spread, P323F variant may have
333 altered phenotypic characteristics, which have contributed to its increased prevalence
334 and thus an active area of investigation. In an attempt to understand the role of this amino
335 acid, our structural modeling of RdRp showed that 323aa is located in the interface
336 domain, which acts as the junction for the interaction of accessory protein (nsp8), required
337 for the polymerase activity [33]. Importantly, P323 of the Wuhan SARS-CoV-2 (Wuhan-
338 Hu1) have mutated to Leucine (P323L) in all D614 variant of spike glycoprotein, which
339 supposedly have higher transmission [25]. Although the role of D61G in combination with
340 P323L of RdRp on viral transmission has not been investigated but co-existence of these
341 mutational changes (D614G and P323L) in almost all predominantly detected variants of
342 SARS-CoV-2 reflect their importance in transmission and pathogenicity. Consequently,
343 higher prevalence of the P323 mutated to 323F (P323F) in variants circulating in the
344 patients of Northern Nevada may suggest the importance of this specific amino acid in
345 virus replication or transmission.
346

347 **DATA AVAILABILITY:**

348 All sequences are available at bio project:

349 https://www.ncbi.nlm.nih.gov/bioproject/657893. All reported data are deposited and

350 available at GISAID: hCoV-19/USA/NV-NSPHL-A (0004-0210)/2020.

351

352 **ACKNOWLEDGEMENTS:**

353 We thank the staff at the Nevada State Public Health Lab (NSPHL) and Southern

354 Nevada, Public Health Laboratory (SNPHL) for providing the RNA extracts from the

355 patient's specimen. This work was supported by University of Nevada, Reno Vice

356 President for Research and Innovation (VPRI), Department of Microbiology &

357 Immunology, UNR School of Medicine, Nevada IDeA Network of Biomedical Research

358 Excellence (INBRE) from the National Institute of General Medical Sciences (GM 103440

359 and GM 104944) from the National Institutes of Health (NIH). The authors wish to

360 acknowledge the support of Research & Innovation and the Office of Information

361 Technology at the University of Nevada, Reno for computing time on the Pronghorn High-

362 Performance Computing Cluster.

363

364 **AUTHOR CONTRIBUTION:**

365 PDH: conceptualization, formal analysis, methodology, writing – original draft preparation,

366 writing – review and editing

367 RLT: conceptualization, formal analysis, methodology, writing – original draft preparation,

368 writing – review and editing

369 XY: formal analysis

370 DPA: conceptualization, funding

371 JRS: formal analysis, review and editing

372 AG: methodology

373 EB: specimen procurement and diagnostic testing

374 HH: specimen procurement and diagnostic testing

375 MP: conceptualization, specimen procurement, diagnostic testing, formal analysis,
376 project administration, writing – review and editing

377 CCR: conceptualization, formal analysis, methodology, project administration, funding,
378 writing – original draft preparation, writing – review and editing

379 SCV: conceptualization, formal analysis, methodology, project administration, funding,
380 writing – review and editing

381

382 **DECLARATIONS:**

383 **Ethics Approval:**

384 Deidentified human specimens (nasal and nasopharyngeal swabs) were used for the
385 extraction of viral RNA all the experiments were done in accordance with guidelines of
386 the University of Nevada, Reno. The University of Nevada, Reno Institutional Review
387 Board (IRB) reviewed this project and determined this study to be EXEMPT FROM IRB
388 REVIEW according to federal regulations and University policy.

389 The Environmental and Biological Safety committee of the University of Nevada, Reno,
390 approved methods and techniques used in this study.

391

392 **Competing Interests:**

393 The authors declare that they have no competing interests with the contents of this article.

394 **REFERENCES:**

395 1. Coronaviridae Study Group of the International Committee on Taxonomy of V (2020)
396 The species Severe acute respiratory syndrome-related coronavirus: classifying 2019-
397 nCoV and naming it SARS-CoV-2. Nat Microbiol 5 (4):536-544. doi:10.1038/s41564-
398 020-0695-z
399 2. Petrosillo N, Viceconte G, Ergonul O, Ippolito G, Petersen E (2020) COVID-19, SARS
400 and MERS: are they closely related? Clin Microbiol Infect 26 (6):729-734.
401 doi:10.1016/j.cmi.2020.03.026
402 3. Zhou P, Yang XL, Wang XG, Hu B, Zhang L, Zhang W, Si HR, Zhu Y, Li B, Huang
403 CL, Chen HD, Chen J, Luo Y, Guo H, Jiang RD, Liu MQ, Chen Y, Shen XR, Wang X,
404 Zheng XS, Zhao K, Chen QJ, Deng F, Liu LL, Yan B, Zhan FX, Wang YY, Xiao GF, Shi
405 ZL (2020) A pneumonia outbreak associated with a new coronavirus of probable bat
406 origin. Nature 579 (7798):270-273. doi:10.1038/s41586-020-2012-7
407 4. Hu D, Zhu C, Ai L, He T, Wang Y, Ye F, Yang L, Ding C, Zhu X, Lv R, Zhu J, Hassan
408 B, Feng Y, Tan W, Wang C (2018) Genomic characterization and infectivity of a novel
409 SARS-like coronavirus in Chinese bats. Emerg Microbes Infect 7 (1):154.
410 doi:10.1038/s41426-018-0155-5
411 5. de Wit E, van Doremalen N, Falzarano D, Munster VJ (2016) SARS and MERS:
412 recent insights into emerging coronaviruses. Nat Rev Microbiol 14 (8):523-534.
413 doi:10.1038/nrmicro.2016.81
414 6. Peiris JS, Lai ST, Poon LL, Guan Y, Yam LY, Lim W, Nicholls J, Yee WK, Yan WW,
415 Cheung MT, Cheng VC, Chan KH, Tsang DN, Yung RW, Ng TK, Yuen KY, group Ss
416 (2003) Coronavirus as a possible cause of severe acute respiratory syndrome. Lancet
417 361 (9366):1319-1325. doi:10.1016/s0140-6736(03)13077-2
418 7. Zaki AM, van Boheemen S, Bestebroer TM, Osterhaus AD, Fouchier RA (2012)
419 Isolation of a novel coronavirus from a man with pneumonia in Saudi Arabia. N Engl J
420 Med 367 (19):1814-1820. doi:10.1056/NEJMoa1211721
421 8. Zhong NS, Zheng BJ, Li YM, Poon, Xie ZH, Chan KH, Li PH, Tan SY, Chang Q, Xie
422 JP, Liu XQ, Xu J, Li DX, Yuen KY, Peiris, Guan Y (2003) Epidemiology and cause of
423 severe acute respiratory syndrome (SARS) in Guangdong, People's Republic of China,
424 in February, 2003. Lancet 362 (9393):1353-1358. doi:10.1016/s0140-6736(03)14630-2

425 9. Kim D, Lee JY, Yang JS, Kim JW, Kim VN, Chang H (2020) The Architecture of
426 SARS-CoV-2 Transcriptome. Cell 181 (4):914-921 e910. doi:10.1016/j.cell.2020.04.011
427 10. Licastro D, Rajasekharan S, Dal Monego S, Segat L, D'Agaro P, Marcello A (2020)
428 Isolation and Full-Length Genome Characterization of SARS-CoV-2 from COVID-19
429 Cases in Northern Italy. J Virol 94 (11). doi:10.1128/JVI.00543-20
430 11. Holland LA, Kaelin EA, Maqsood R, Estifanos B, Wu LI, Varsani A, Halden RU,
431 Hogue BG, Scotch M, Lim ES (2020) An 81-Nucleotide Deletion in SARS-CoV-2 ORF7a
432 Identified from Sentinel Surveillance in Arizona (January to March 2020). J Virol 94 (14).
433 doi:10.1128/JVI.00711-20
434 12. Wu F, Zhao S, Yu B, Chen YM, Wang W, Song ZG, Hu Y, Tao ZW, Tian JH, Pei
435 YY, Yuan ML, Zhang YL, Dai FH, Liu Y, Wang QM, Zheng JJ, Xu L, Holmes EC, Zhang
436 YZ (2020) A new coronavirus associated with human respiratory disease in China.
437 Nature 579 (7798):265-269. doi:10.1038/s41586-020-2008-3
438 13. Davidson AD, Williamson MK, Lewis S, Shoemark D, Carroll MW, Heesom KJ,
439 Zambon M, Ellis J, Lewis PA, Hiscox JA, Matthews DA (2020) Characterisation of the
440 transcriptome and proteome of SARS-CoV-2 reveals a cell passage induced in-frame
441 deletion of the furin-like cleavage site from the spike glycoprotein. Genome Med 12
442 (1):68. doi:10.1186/s13073-020-00763-0
443 14. Walls AC, Park YJ, Tortorici MA, Wall A, McGuire AT, Veesler D (2020) Structure,
444 Function, and Antigenicity of the SARS-CoV-2 Spike Glycoprotein. Cell 181 (2):281-292
445 e286. doi:10.1016/j.cell.2020.02.058
446 15. Bolger AM, Lohse M, Usadel B (2014) Trimmomatic: a flexible trimmer for Illumina
447 sequence data. Bioinformatics 30 (15):2114-2120. doi:10.1093/bioinformatics/btu170
448 16. Langmead B, Salzberg SL (2012) Fast gapped-read alignment with Bowtie 2. Nat
449 Methods 9 (4):357-359. doi:10.1038/nmeth.1923
450 17. Picard-Toolkit. (2019) [cited 17 Aug 2020]. In: Github [Internet] Available:
451 http://broadinstitute.github.io/picard
452 18. Garrison E, Marth G (2012) Haplotype-based variant detection from short-read
453 sequencing. arXiv [q-bioGN] Available: http://arxiv.org/abs/1207.3907
454 19. Garrison E (2019) Vcflib: A C++ library for parsing and manipulating VCF files.
455 Available: https://githubcom/vcflib/vcflib

456 20. Li H (2011) A statistical framework for SNP calling, mutation discovery, association
457 mapping and population genetical parameter estimation from sequencing data.
458 Bioinformatics 27 (21):2987-2993. doi:10.1093/bioinformatics/btr509
459 21. Elbe S, Buckland-Merrett G (2017) Data, disease and diplomacy: GISAID's
460 innovative contribution to global health. Glob Chall 1 (1):33-46. doi:10.1002/gch2.1018
461 22. Nextstrain. (2020) Genomic epidemiology of novel coronavirus - Global
462 subsampling. In: Nextstrainorg [Internet] 15 Jul 2020 [cited 15 Jul 2020] Available:
463 https://nextstrain.org/ncov/global/2020-07-15?d=tree&l=clock&legend=closed
464 23. Hadfield J, Megill C, Bell SM, Huddleston J, Potter B, Callender C, Sagulenko P,
465 Bedford T, Neher RA (2018) Nextstrain: real-time tracking of pathogen evolution.
466 Bioinformatics 34 (23):4121-4123. doi:10.1093/bioinformatics/bty407
467 24. Chen J, Malone B, Llewellyn E, Grasso M, Shelton PMM, Olinares PDB, Maruthi K,
468 Eng ET, Vatandaslar H, Chait BT, Kapoor TM, Darst SA, Campbell EA (2020) Structural
469 Basis for Helicase-Polymerase Coupling in the SARS-CoV-2 Replication-Transcription
470 Complex. Cell. doi:10.1016/j.cell.2020.07.033
471 25. Korber B, Fischer WM, Gnanakaran S, Yoon H, Theiler J, Abfalterer W, Hengartner
472 N, Giorgi EE, Bhattacharya T, Foley B, Hastie KM, Parker MD, Partridge DG, Evans
473 CM, Freeman TM, de Silva TI, Sheffield C-GG, McDanal C, Perez LG, Tang H, Moon-
474 Walker A, Whelan SP, LaBranche CC, Saphire EO, Montefiori DC (2020) Tracking
475 Changes in SARS-CoV-2 Spike: Evidence that D614G Increases Infectivity of the
476 COVID-19 Virus. Cell 182 (4):812-827 e819. doi:10.1016/j.cell.2020.06.043
477 26. Nextclade (2020) [cited 17 Aug 2020]. Available: https://cladesnextstrainorg
478 27. Matranga CB, Andersen KG, Winnicki S, Busby M, Gladden AD, Tewhey R,
479 Stremlau M, Berlin A, Gire SK, England E, Moses LM, Mikkelsen TS, Odia I, Ehiane PE,
480 Folarin O, Goba A, Kahn SH, Grant DS, Honko A, Hensley L, Happi C, Garry RF,
481 Malboeuf CM, Birren BW, Gnirke A, Levin JZ, Sabeti PC (2014) Enhanced methods for
482 unbiased deep sequencing of Lassa and Ebola RNA viruses from clinical and biological
483 samples. Genome Biol 15 (11):519. doi:10.1186/PREACCEPT-1698056557139770
484 28. Briese T, Kapoor A, Mishra N, Jain K, Kumar A, Jabado OJ, Lipkin WI (2015)
485 Virome Capture Sequencing Enables Sensitive Viral Diagnosis and Comprehensive
486 Virome Analysis. mBio 6 (5):e01491-01415. doi:10.1128/mBio.01491-15

487 29. O'Flaherty BM, Li Y, Tao Y, Paden CR, Queen K, Zhang J, Dinwiddie DL, Gross
488 SM, Schroth GP, Tong S (2018) Comprehensive viral enrichment enables sensitive
489 respiratory virus genomic identification and analysis by next generation sequencing.
490 Genome Res 28 (6):869-877. doi:10.1101/gr.226316.117
491 30. Paden CR, Tao Y, Queen K, Zhang J, Li Y, Uehara A, Tong S (2020) Rapid,
492 Sensitive, Full-Genome Sequencing of Severe Acute Respiratory Syndrome
493 Coronavirus 2. Emerg Infect Dis 26 (10). doi:10.3201/eid2610.201800
494 31. Paskey AC, Frey KG, Schroth G, Gross S, Hamilton T, Bishop-Lilly KA (2019)
495 Enrichment post-library preparation enhances the sensitivity of high-throughput
496 sequencing-based detection and characterization of viruses from complex samples.
497 BMC Genomics 20 (1):155. doi:10.1186/s12864-019-5543-2
498 32. Xiao M, Liu X, Ji J, Li M, Li J, Yang L, Sun W, Ren P, Yang G, Zhao J, Liang T, Ren
499 H, Chen T, Zhong H, Song W, Wang Y, Deng Z, Zhao Y, Ou Z, Wang D, Cai J, Cheng
500 X, Feng T, Wu H, Gong Y, Yang H, Wang J, Xu X, Zhu S, Chen F, Zhang Y, Chen W, Li
501 Y, Li J (2020) Multiple approaches for massively parallel sequencing of SARS-CoV-2
502 genomes directly from clinical samples. Genome Med 12 (1):57. doi:10.1186/s13073-
503 020-00751-4
504 33. Kirchdoerfer RN, Ward AB (2019) Structure of the SARS-CoV nsp12 polymerase
505 bound to nsp7 and nsp8 co-factors. Nat Commun 10 (1):2342. doi:10.1038/s41467-019-
506 10280-3
507
508
509 **FIGURE LEGENDS:**
510 **Figure 1. Workflow of SARS-CoV-2 genome sequencing and analysis from**
511 **nasopharyngeal patient specimens in Nevada.** (A) RNA was extracted from Nasal or
512 Nasopharygeal (NP) swabs taken from patients in Nevada and first used to determine the
513 presence of SARS-CoV-2 genomes by RT-qPCR. Next generation sequencing (NGS)
514 libraries were prepared from positive specimens, this included steps for ribosomal RNA
515 depletion and SARS-CoV-2 enrichment. Subsequent libraries were pooled and used for

516 whole genome sequencing at the Nevada Genomics Center on the Illumina NextSeq 500
517 instrument. FASTQ files were aligned to the reference genome, and analyzed to
518 determine nucleotide variation and phylogenetic relationship. (B) A total of 200 specimens
519 were sequenced, of which 174 had over 99% coverage of the SARS-CoV-2 genome.
520 This included 133 patient specimens from Northern Nevada, 40 from Southern Nevada
521 and 1 specimen that was re-sequenced. (C) Correlation between RT-qPCR Ct value and
522 the percentage of coverage in the whole genome sequencing after trimming and
523 alignment. (D) Nucleotide variants across the SARS-CoV-2 genome in the 173 specimens
524 from Nevada from March 6 to June 5.
525
526 **Figure 2. Distribution of D614G in Nevada and comparison with the United States**
527 **and global proportion.** (A) Cumulative frequency of D614G in 173 patient specimens
528 from Nevada from March 6 to June 5, 2020 (D614 is indicated by teal, G614 is indicated
529 by yellow). Pie charts depict the cumulative proportion up to the indicated time point
530 (March 15, April 1, May 1, June 5). The total number of specimens included at each time
531 point is specified below each pie chart. Effective dates of emergency orders and
532 regulatory responses to SARS-CoV-2 spread in Nevada are indicated on the frequency
533 graph time axis. (B) Proportion of D614G in the United States from March 6 to June 5,
534 specimens from Nevada are divided in the geographic area that they originated from,
535 Northern Nevada (N-NV) includes 133 specimens from Washoe County, Carson-Tahoe,
536 and other northern counties, and Southern Nevada (S-NV) includes 40 specimens from
537 Clark County. (C) Global proportion of D614G in the shown regions during the same time

538 period from a subsampling of sequences deposited in Nextstrain.org. The size of the pie
539 chart corresponds to the relative specimen number for each region.
540
541 **Figure 3. Distribution of SARS-CoV-2 clades in Nevada.** (A) Cumulative frequency of
542 SARS-CoV-2 clades in 173 patient specimens from Nevada during March 6 to June 5.
543 The five clades are colored 19A (blue), 19B (teal), 20A (green), 20B (yellow) and 20C
544 (orange). Pie charts depict the cumulative proportion up to the indicated time point (March
545 15, April 1, May 1, June 5). The total number of specimens included at each time point is
546 specified below each pie chart. Dates of emergency orders and regulations meant to slow
547 the spread of SARS-CoV-2 in Nevada are indicated on the time scale of the frequency
548 graph. (B) Circular dendrogram depicting clades from Nevada specimens. (C) Pie chart
549 of the clades from northern Nevada (N-NV), southern Nevada (S-NV) and the United
550 States. (D) Pie charts show the proportion of clades from global regions during the same
551 time period from a subsampling of sequences deposited in Nextstrain.org. The size of the
552 pie chart corresponds to the relative specimen number for each region.
553
554 **Figure 4. Distribution of P323L/F (nsp12, RdRp) in Nevada.** (A) Cumulative frequency
555 of P323L/F (nsp12, RdRp) in 173 patient specimens from Nevada during March 6 to June
556 5. The amino acid at position 323 is indicated by teal for proline (P), yellow for leucine (L)
557 and blue for phenylalanine (F). Pie charts depict the cumulative proportion up to the
558 indicated time point (March 15, April 1, May 1, June 5). The total number of specimens
559 included at each time point is specified below each pie chart. Dates of emergency orders
560 and regulations meant to slow the spread of SARS-CoV-2 in Nevada are indicated on the

561 time scale of the frequency graph. (B) Circular dendrogram representing the distribution
562 of amino acid change at residue 323 of nsp12 from a global subsampling of sequences
563 deposited in Nextstrain.org from March 6 to June 5, the larger dots indicate specimens
564 from Nevada. (C) Pie chart indicating the ratio of P/L/F in Northern NV and Southern NV
565 specimens from this study. (D) Proportion of P323L/F from a subsampling of sequences
566 deposited in Nextstrain.org for the United States and (E) global regions from March 6 to
567 June 5. The size of the pie chart corresponds to the relative specimen number for each
568 region.
569
570 **Figure 5. Structure of SARS-CoV-2 nsp12 (RdRp) P323L/F.** (a) Diagram depicting
571 ORF1b genomic location and encoded proteins. Below the linear protein schematic of
572 nsp12 specific nucleotide variants at position 14,407 and 14,408 and the resulting amino
573 acid changes are indicated. (b) SARS-CoV-2 replicase complex modeled from 6XEZ
574 template. This model includes nsp12, nsp7, nsp8, nsp13, ligands (ZN, Mg), the template
575 and product strand of RNA. P323L/F within the interface domain of nsp12 is located at
576 the left side of the complex. (c) Model nsp12 showing P323L/F within the interface
577 domain. Residue 323 is shown with either P, L or F and amino acids with side chains
578 within 5 Å of residue 323 are depicted as sticks in the cartoon model.
579
580 **Figure 6. Distribution of nucleotide variant 379C>A.** (a) Green line at the far-left end
581 of the genome denoted nucleotide position 379 of nsp1. (b) Circular dendrogram of global
582 subsample of sequences from Nextstrain.org with NV specimens indicated by larger dots.
583 (c) Pie chart indicating the proportion of sequences with either the cytidine (C) or

584 adenosine (A) at position 379 from the Nevada specimens. Subsample of sequences from
585 Nextstrain.org were used to generate the proportion of 379C>A in (d) the indicated states
586 within the U.S. and (e) internationally. The size of the pie chart corresponds to the relative
587 specimen number for each region.
588
589 **SUPPLEMENTARY FIGURES**
590 **Figure S1. Alignment of SARS-CoV-2 sequences from NV patient's specimens.**
591 SARS-CoV-2 sequences from patient specimen were aligned together with the original
592 COVID-19 sequence from Wuhan, NC_045512.2, using multiple sequences alignment
593 tool MUSCLE 3.8.31. The aligned sequences were sorted based on number of Ns in
594 each sequence from the smallest to the largest. The sorted alignment file in aln format
595 was uploaded to the web portal of NCBI Multiple Sequence Alignment Viewer, Version
596 1.15.0, for visualization.
597
598 **Figure S2. Dendrogram of Nevada specimens in context of other sequenced**
599 **specimens.** (a) Nucleotide mutation clock from Nextstrain.org with the SARS-CoV-2
600 genome isolated from Washington (USA/WA 1/2020) on January 24th and first specimen
601 from Nevada (A0004) on March 5th indicated in red. (b) Circular dendrogram of Nevada
602 specimens from March 6th to June 5th positioned within a subsample of global sequences
603 from Nextstrain.org during the same time period, the larger dots indicate specimens from
604 Nevada. The five clades are colored 19A (blue), 19B (teal), 20A (green), 20B (yellow) and
605 20C (orange).
606

Figure S3. Global distribution of clades from March 6th to June 5th. Pie charts depict the proportion of the clades within (a) four main areas in Nevada, these include 91 specimens from Washoe county (upper left), 23 specimens from Carson-Tahoe (middle left), 40 specimens from Clark county (bottom right), and 19 from rural Nevada (middle). The five clades are colored 19A (blue), 19B (teal), 20A (green), 20B (yellow) and 20C (orange). (b) Pie chart of the clades in each indicated country from March 6th to June 5th generated from a subsampling of sequences deposited in Nextstrain.org. The size of the pie chart corresponds to the relative specimen number for each region.

630

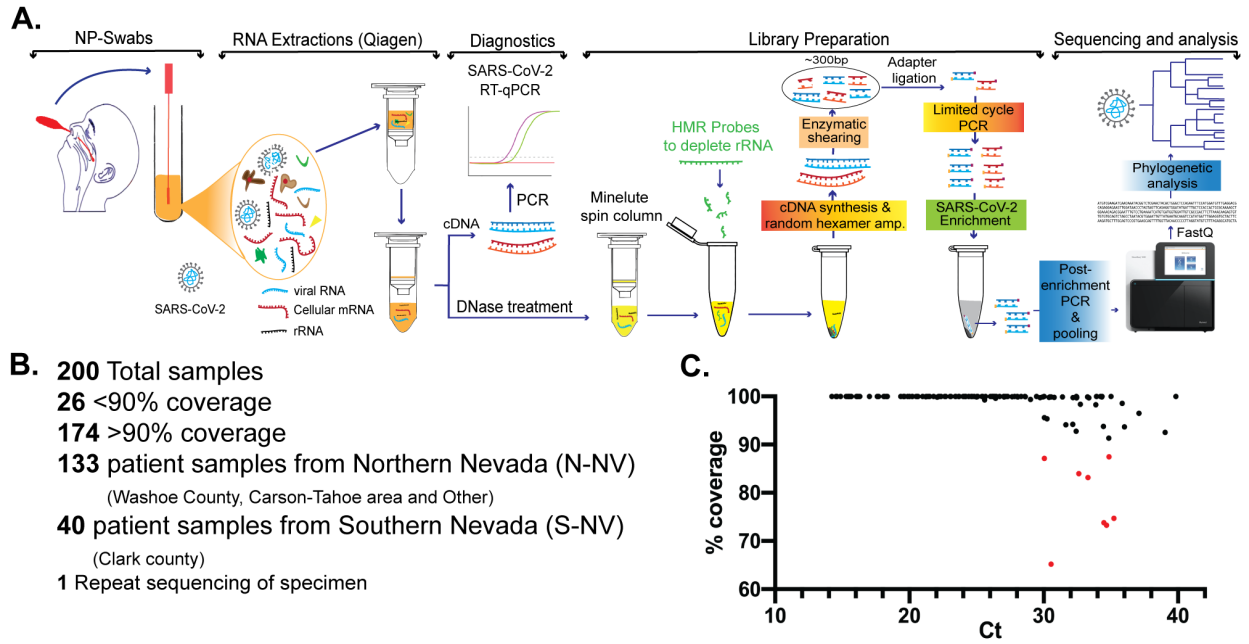

B. **200** Total samples
26 <90% coverage
174 >90% coverage
133 patient samples from Northern Nevada (N-NV)
(Washoe County, Carson-Tahoe area and Other)
40 patient samples from Southern Nevada (S-NV)
(Clark county)
1 Repeat sequencing of specimen

D.

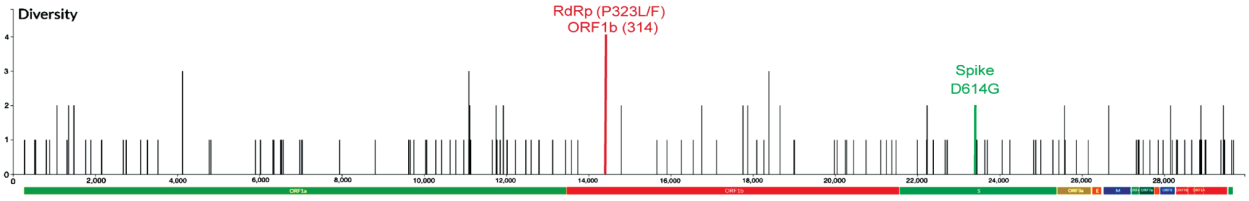

631

632

633

634

635

636

637

638

639

640

641

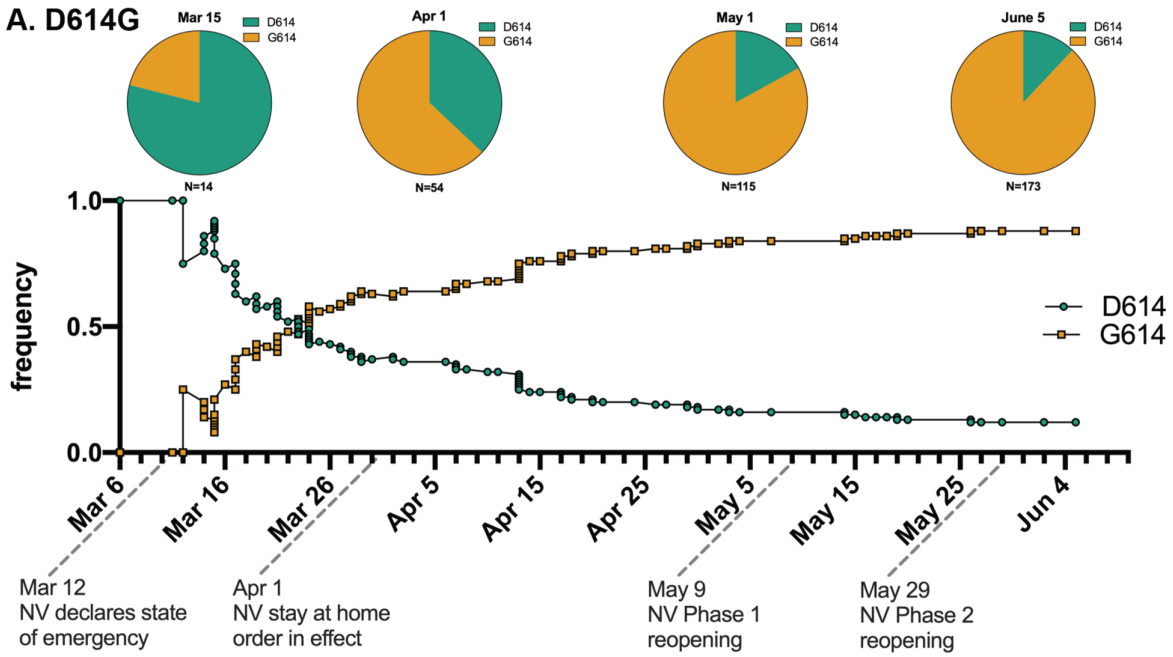

B. NV data March 6- June 5, 2020

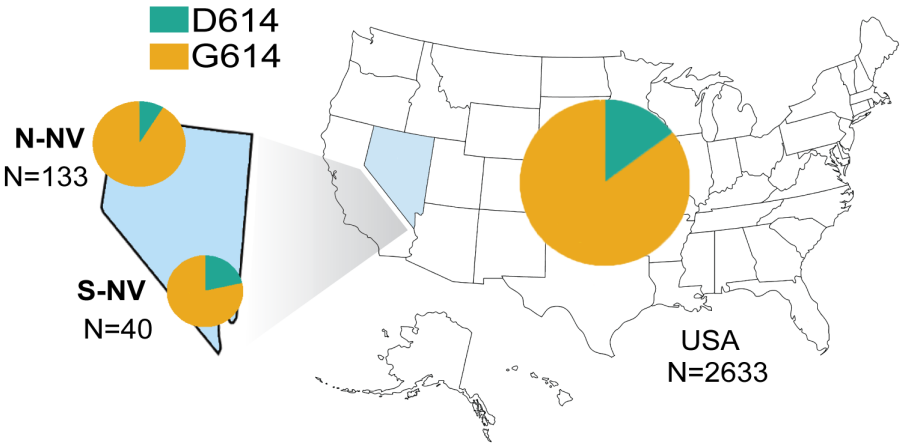

C. Global data March 6- June 5, 2020

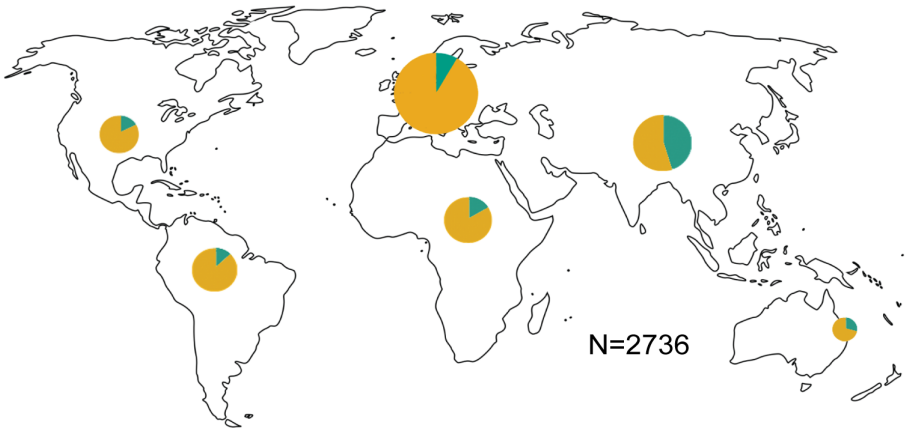

642

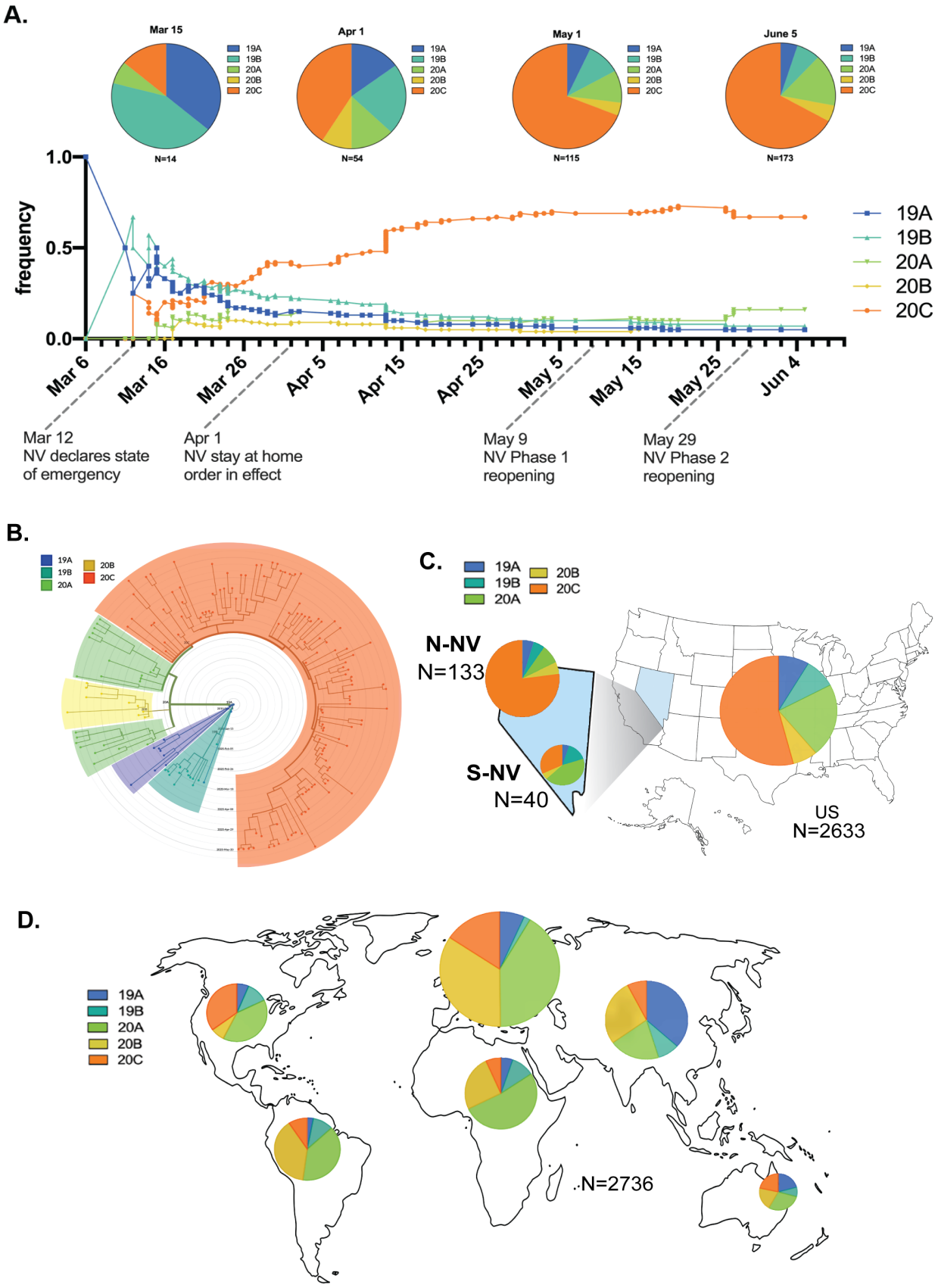
A.
Mar 15
Apr 1
May 1
June 5
19A
19B
20A
20B
20C
N=14
N=54
N=115
N=173
1.0
0.5
0.0
frequency
Mar 6
Mar 16
Mar 26
Apr 5
Apr 15
Apr 25
May 5
May 15
May 25
Jun 4
Mar 12
NV declares state
of emergency
Apr 1
NV stay at home
order in effect
May 9
NV Phase 1
reopening
May 29
NV Phase 2
reopening
B.
C.
N-NV
N=133
S-NV
N=40
US
N=2633
D.
N=2736

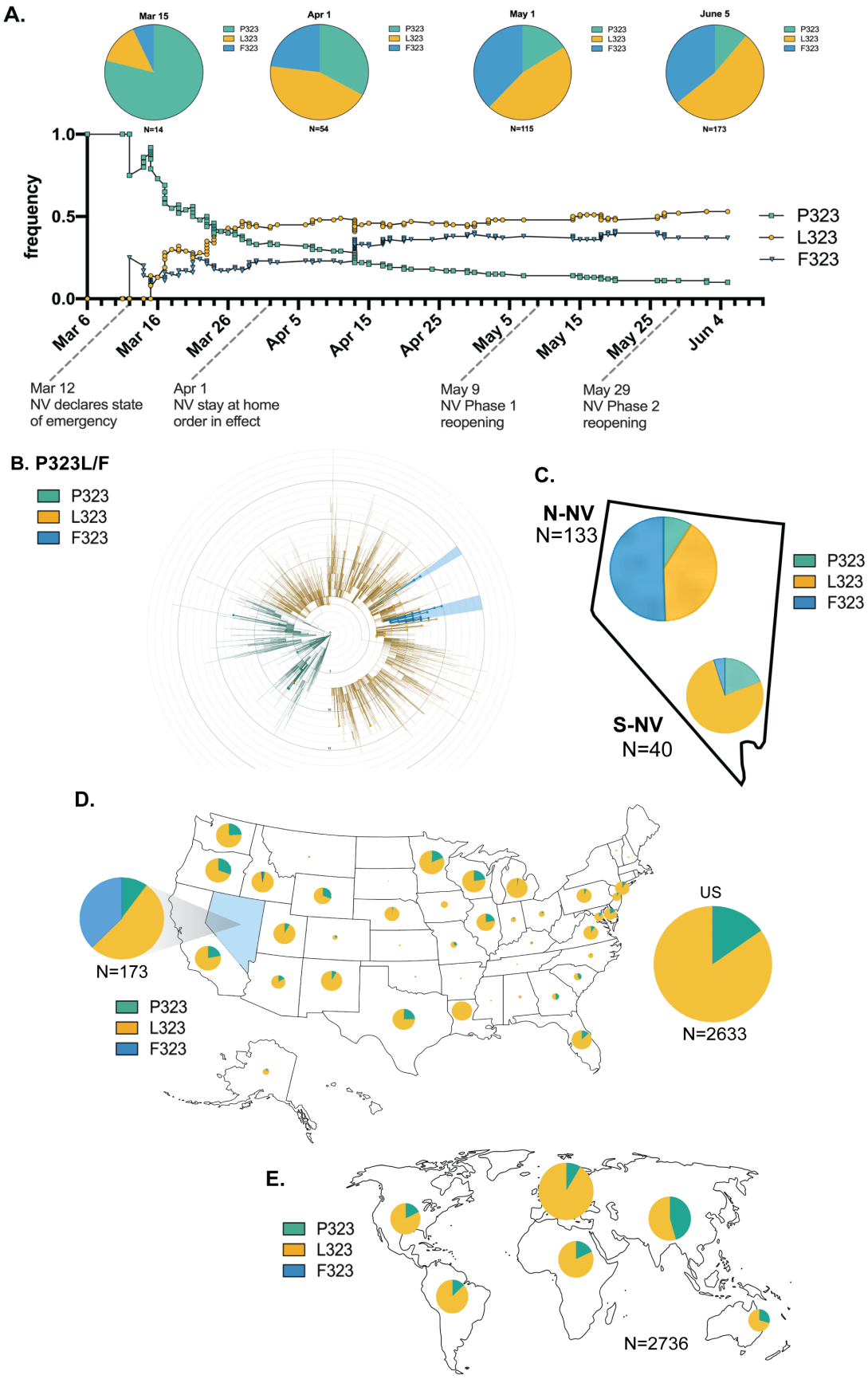
A.
Mar 15
Apr 1
May 1
June 5
P323
L323
F323
N=14
N=54
N=115
N=173
frequency
1.0
0.5
0.0
Mar 6
Mar 16
Mar 26
Apr 5
Apr 15
Apr 25
May 5
May 15
May 25
Jun 4
Mar 12
NV declares state of emergency
Apr 1
NV stay at home order in effect
May 9
NV Phase 1 reopening
May 29
NV Phase 2 reopening
B. P323L/F
C.
N-NV
N=133
S-NV
N=40
D.
N=173
US
N=2633
E.
N=2736

644

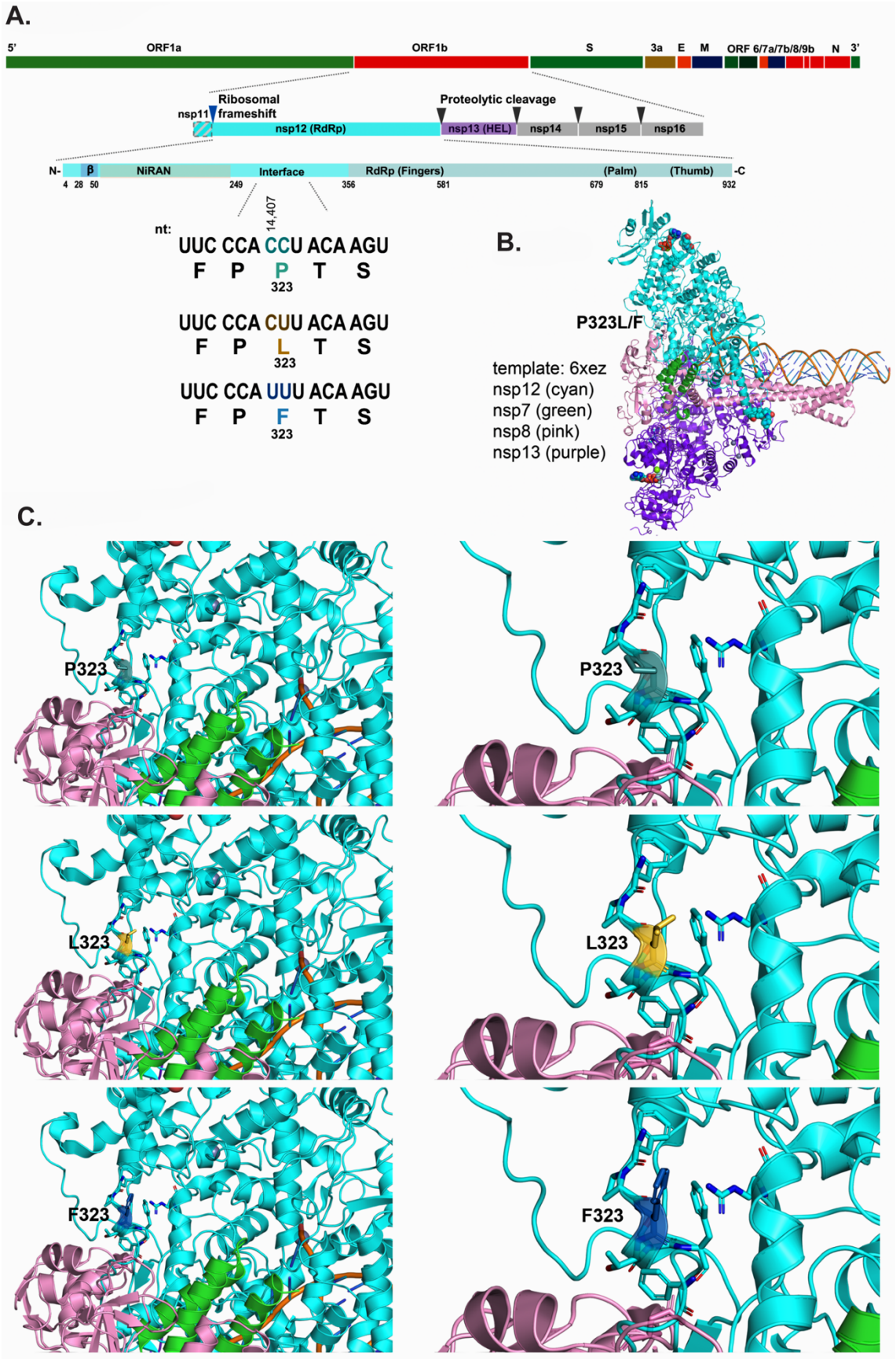
A.
5'
ORF1a
ORF1b
S
3a
E
M
ORF 6/7a/7b/8/9b
N
3'
Ribosomal frameshift
nsp11
Proteolytic cleavage
nsp12 (RdRp)
nsp13 (HEL)
nsp14
nsp15
nsp16
N-
β
NiRAN
Interface
RdRp (Fingers)
(Palm)
(Thumb)
-C
4 28 50
249
356
581
679
815
932
14,407
nt:
UUC CCA CCU ACA AGU
F P P T S
323
UUC CCA CUU ACA AGU
F P L T S
323
UUC CCA UUU ACA AGU
F P F T S
323
B.
P323L/F
template: 6xez
nsp12 (cyan)
nsp7 (green)
nsp8 (pink)
nsp13 (purple)
C.
P323
P323
L323
L323
F323
F323

645

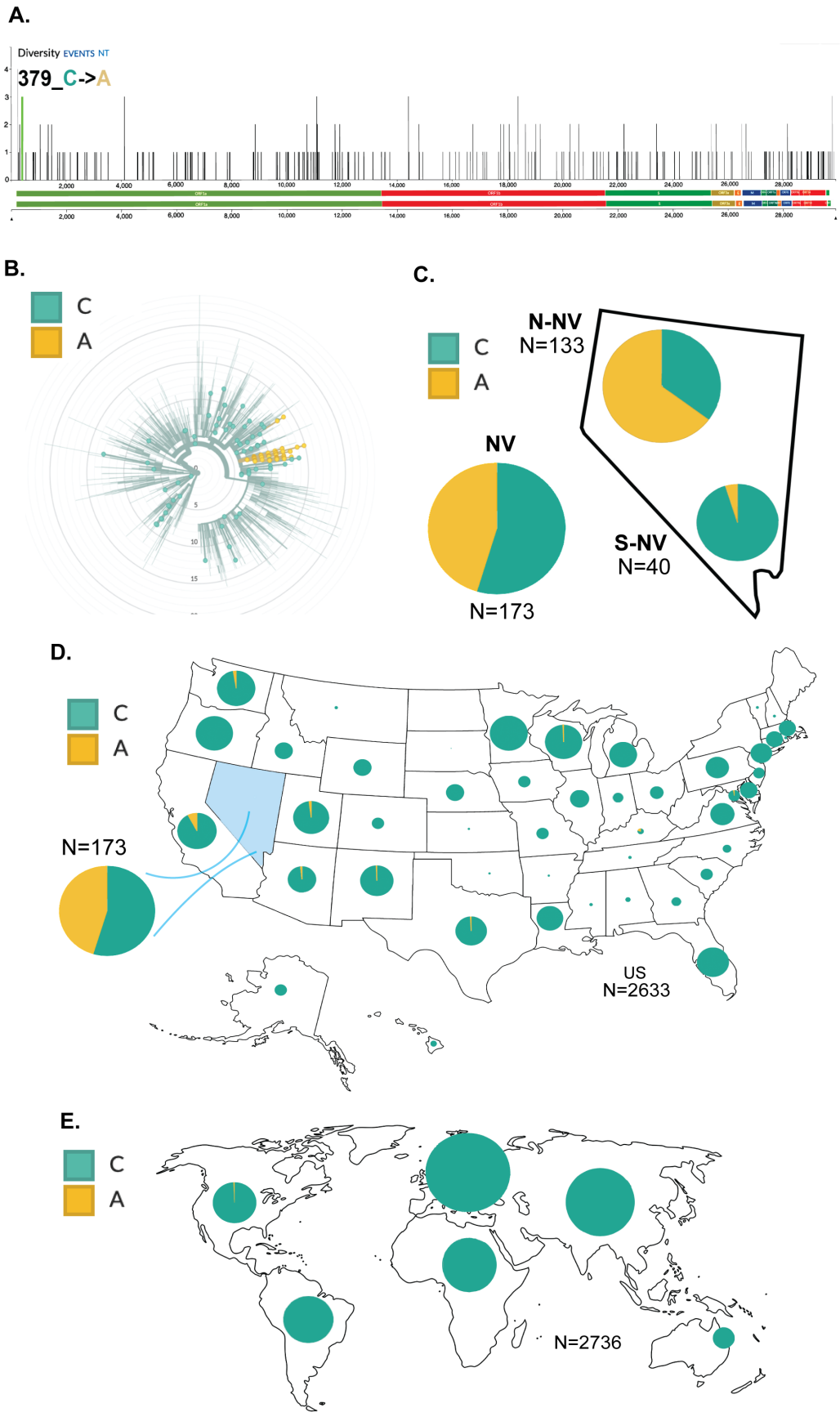
A.
Diversity EVENTS NT
379_C->A
B.
C
A
C.
C
A
N-NV
N=133
NV
N=173
S-NV
N=40
D.
C
A
N=173
US
N=2633
E.
C
A
N=2736

646

SUPPLEMENTARY INFORMATION:

Figure S1: Alignment of SARS-CoV-2 sequences from NV patient's specimens.

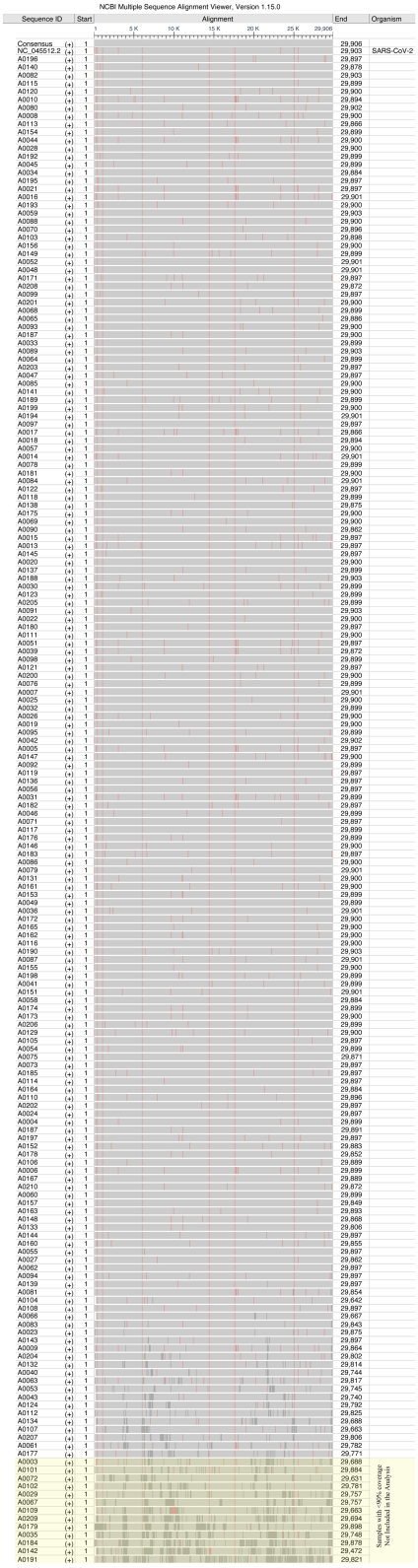

Figure S2. Dendrogram of Nevada specimens in context of other sequenced specimens. (a) Nucleotide mutation clock from Nextstrain.org with the SARS-CoV-2 genome isolated from Washington (USA/WA 1/2020) on January 24th and first specimen from Nevada (A0004) on March 5th indicated in red. (b) Circular dendrogram of Nevada specimens from March 6th to June 5th positioned within a subsample of global sequences from Nextstrain.org during the same time period, the larger dots indicate specimens from Nevada. The five clades are colored 19A (blue), 19B (teal), 20A (green), 20B (yellow) and 20C (orange).

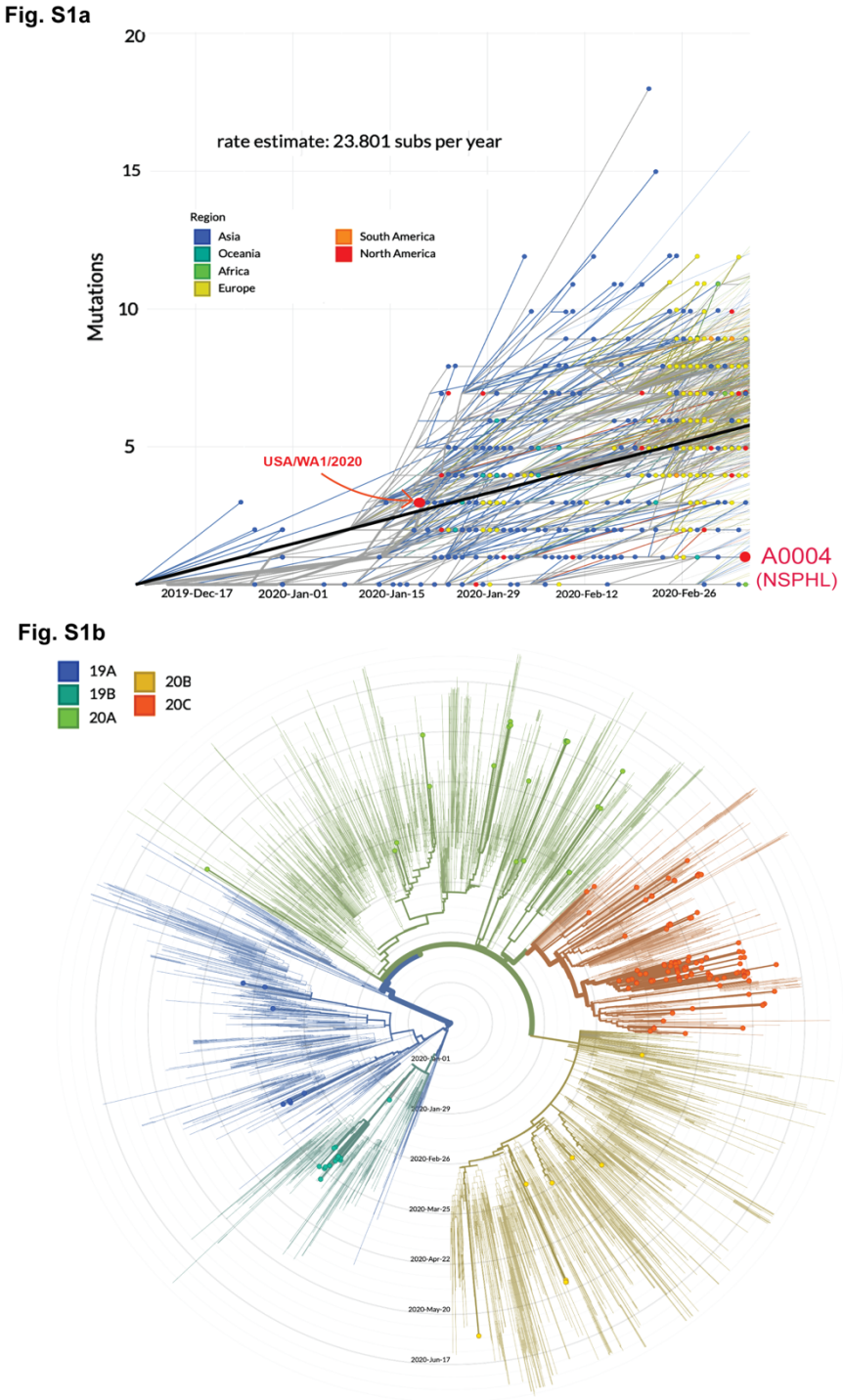

Figure S3. Global distribution of clades from March 6th to June 5th. Pie charts depict the proportion of the clades within (a) four main areas in Nevada, these include 91 specimens from Washoe county (upper left), 23 specimens from Carson-Tahoe (middle left), 40 specimens from Clark county (bottom right), and 19 from rural Nevada (middle). The five clades are colored 19A (blue), 19B (teal), 20A (green), 20B (yellow) and 20C (orange). (b) Pie chart of the clades in each indicated country from March 6th to June 5th generated from a subsampling of sequences deposited in Nextstrain.org. The size of the pie chart corresponds to the relative specimen number for each region.

Fig. S2a

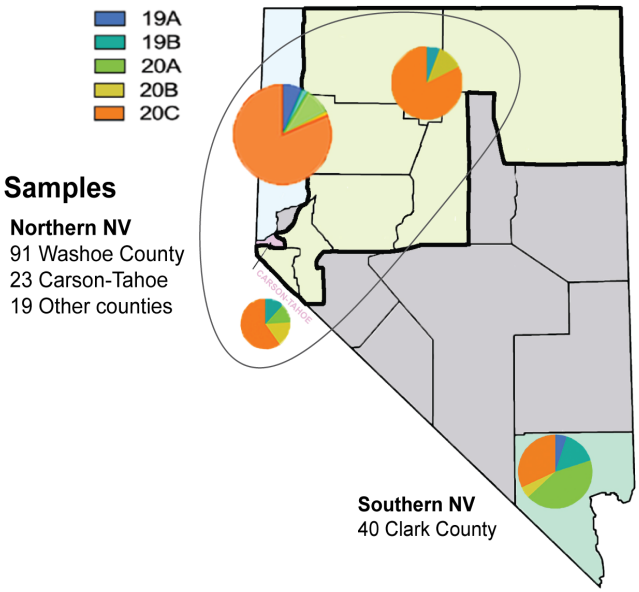
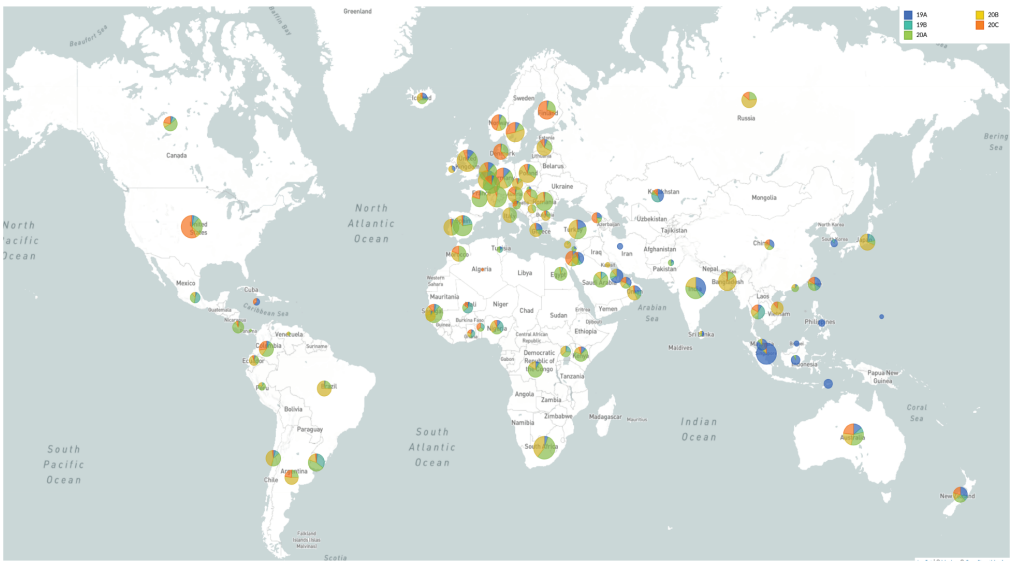
Fig. S2b